Results in Physics 24 (2021) 104113

Contents lists available at ScienceDirect

Results in Physics

journal homepage: www.elsevier.com/locate/rinp

Interactions of pulses produced by two- mode resonant nonlinear Schrodinger equations

H.I. Abdel-Gawad [a,*], Choonkil Park [b,*]

[a] Department of Mathematics, Faculty of Science, Cairo University, Egypt
[b] Research Institute for Natural Sciences, Hanyang University, Seoul 04763, South Korea

ARTICLE INFO

Keywords:
Two-mode
Resonant
Schrodinger equation
Pulses shapes
Colliding dynamics

ABSTRACT

Single resonant nonlinear Schrodinger equation RNLSE has wide applications in sciences. It describes the transient state between self-focusing and self-defocusing polarization. This motivated researchers to study and investigate the physical characteristics behind. Here, we are concerned with analyzing the solutions of two-mode RNLSE which may reveal complex phenomena. Novel shapes of pulses propagation in optical fibers are shown Further, the colliding dynamics of waves are inspected. The different characteristics of pulses are defined and interpreted. These features are studied via finding the exact solutions of the two modes RNLSE. These solutions are obtained. by using the unified method. It is found that the criteria of the polarization of the two modes may be, mutual, or of the same polarization. Which depends on the crucial values of the coefficients of the quantum potential. Also, it is shown that the propagation of pulses exhibits multiple-geometric structures.Which are complex chirped, M-W-shaped pulses, rhombus (diamond) and tun able conoidal pulses. These are novel features of pulses propagation.The spectral characteristics show a variety of some important results. Here, it is inspected that the collision is elastic.

Introduction

Diverse formulation of nonlinear Schrodinger equations NLSEs were the objectives of huge number of research works in the literature. These equations are integrable when the real and imaginary parts are taken linearly dependent [1]. Recent works [2,3] show that the solutions of NLSEs with Kerr nonlinearity describe pulses that exhibit common shapes. A class of an infinite number of the stable bright and dark soliton, was obtained [3] are. Non local NLSE was introduced in [4]. In [5], the generalized Darboux transformation was performed to solve NLSE. The dynamics of rogue waves of multiple orders were presented, Some relevant properties are remarked. It was found that NLSEs possess an infinite number of conservation laws [6]. The solutions of NLSE coupled with Maxwell equations have shown standing waves, which are non-radially symmetric [6].The analytic solutions of thel NLSE under periodic boundary conditions, in the case of the self-focusing Kerr medium, were presented in [7]. NLSEs may take may have a diversity of forms. They can describe optical wave propagation in highly dispersive medium. It was shown that pulses propagation may lead to a variant refractive index Kerr medium [1]. Which, in turn may produce a phase shift in the pulse [8] In mathematical terms, an extra nonlinear correction to the NLSE is considered. Indeed, for nonlinear short-pulse propagation in optical fibers, the governing equation has to include the pulse envelope derivative.Thus, symmetric pulse will undergo an asymmetric self-phase modulation [9]. Further, the effect of self-phase modulation of a pulse propagation was analyzed in [10]. Tun-able delays in optical fiber via a dispersive one or double stages of broadening the spectral content, are observed [11]. It is found that the RNLSE results when describing the transmission of uni-axial waves in a cold collisionless plasma subject to a transverse magnetic field [11]. RNLAEoccupied a wide area of research in the literature [12–25].In those works, the solutions obtained are mainly bright (dark) soliton or lumps.Also, further relevant research work on RNLSE were carried in the literature [26–38]. In[26] the self-similar pulse propagation of optical pulses, for RNLSE with time dependent coefficients, was studied. In the present work different geometric shapes of pulses are inspected. In [27], The resonant pulses are analytically investigated in terms of Gaussian beams, Airy beams, and periodic beams. While in [28], the conservation laws are constructed. In [29], exact solutions were found with varying the refractive index. In [30,31], exact solutions were obtained when the coefficients are time dependent. In [32,33], the modulation instability was studied. In [24] exact solutions were obtained in the presence of

* Corresponding authors.
E-mail address: baak@hanyang.ac.kr (C. Park).

https://doi.org/10.1016/j.rinp.2021.104113
Received 28 February 2021; Received in revised form 16 March 2021; Accepted 20 March 2021
Available online 2 April 2021

external periodic force. Further relevant works in this area were carried in the literature [43–48].

In the present work, we study the TM-RNLSE, which was not considered in the literature, and it is shown that novel shapes; M-W and diamond shapes of pulses propagation, are observed.

The model equations

The single RNLSE reads

$$ip(x,t)_t+\alpha p(x,t)_{xx}+\lambda|p(x,t)|^2p(x,t)-\beta\frac{|p(x,t)|_{xx}}{|p(x,t)|}p(x,t)=0,(x,t)\in\mathbb{R}\times\mathbb{R}^+ \tag{1}$$

We mention that when $\beta=0$, (1) reduces to the conventional NLSE, where α is the dispersion coefficient and λ is the refractive index that stands to self-focusing or self-defocusing polarization when $\lambda>0$ or $\lambda<0$ respectively. Thus when $\beta\neq 0$, (1) describes the pulses propagation in an intermediate state between self-focusing and self-defocusing. The last term stands for quantum potential. Which is observed in the propagation of chiral solitons in quantum hall-effect [26]. The mentioned potential was introduced in [27]. The Eq. (1) may be considered as the response of a resonance- medium to an action of a normal wave with complex amplitude. Further, it can be recast to Madeluing fluid equations [28]. The two-mode RNLSE, (TM- RNLSE), is

$$\begin{aligned}&ip(x,t)_t+\alpha_1p(x,t)_{xx}+\lambda_1|\psi(x,t)|^2p(x,t)-\beta_1\frac{|\varphi(x,t)|_{xx}}{|\varphi x,t)|}p(x,t)=0,\\&i\psi(x,t)_t+\alpha_2\psi(x,t)_{xx}+\lambda_2|p(x,t)|^2\psi(x,t)-\beta_2\frac{|\psi(x,t)|_{xx}}{\psi(x,t)|}\psi(x,t)=0,(x,t)\in\mathbb{R}\times\mathbb{R}^+,\end{aligned} \tag{2}$$

where p and q are complex functions, x and t represent the normalized displacement ant time variables.

The TM-RNLSE in (2) leads to affect the pulses propagation in optical fibers. That is, on the characteristic parameters.Thus, we are led to identify these physical parameters that describe the pulses propagation in such a complex medium. We write

$$p(x,t)=|p(x,t)|e^{i(\overline{k_1}x-\overline{\omega_1 t})},\quad \varphi(x,t)=|\varphi(x,t)|e^{i(\overline{k_2}x-\overline{\omega_2 t})}, \tag{3}$$

where $|.|$stands for the intensity. $\overline{k}$ and $\overline{\omega}$ are the wave number and frequency which are defined in

$$\begin{aligned}&\overline{k_1}=\frac{\int\int_{\mathbb{R}\times\mathbb{R}^+}|p(x,t)_x|dx\,dt}{\int\int_{\mathbb{R}\times\mathbb{R}^+}|p(x,t)|dx\,dt},\quad \overline{\omega_1}=\frac{\int\int_{R\times\mathbb{R}^+}|p(x,t)_t|dx\,dt}{\int\int_{\mathbb{R}\times\mathbb{R}^+}|p(x,t)|dx\,dt}.\\&\overline{k_2}=\frac{\int\int_{\mathbb{R}\times\mathbb{R}^+}|\varphi(x,t)_x|dx\,dt}{\int\int_{\mathbb{R}\times\mathbb{R}^+}|\varphi(x,t)|dx\,dt},\quad \overline{\omega_2}=\frac{\int\int_{R\times\mathbb{R}^+}|\varphi(x,t)_t|dx\,dt}{\int\int_{\mathbb{R}\times\mathbb{R}^+}|\varphi(x,t)|dx\,dt}\end{aligned} \tag{4}$$

The spectrum is defined by

$$P(k_0,t)=\frac{1}{2\pi}\int_R\varphi(x,t)e^{-ik_0x}dx.,\quad Q(k_0,t)=\frac{1}{2\pi}\int_R\psi(x,t)e^{-ik_0x}dx. \tag{5}$$

Now, we find the exact solutions of (2). To this end, we introduce the following transformations [29].

$$p(x,t)=(u_1(x,t)+iv_1(x,t))e^{i(k_1x-\omega_1t)},\quad \psi(x,t)=(u_2(x,t)+iv_2(x,t))e^{i(k_2x-\omega_2t)}. \tag{6}$$

It is worthy to mention that the colliding dynamics can be inspected, whenever the different pulses structures are determined.

By inserting (6) into (2), we get the following equations for the real and imaginary parts of (2);

$$\begin{aligned}&u_1^4(-k_1^2\alpha_1+\omega_1)+\lambda_1u_1(u_2^2+v_2^2)+v_1^4(-k_1^2\alpha_1+\omega_1+\lambda_1(u_2^2+v_2^2))\\&-\beta_1v_1^2u_{1x}\widehat{2}-u_1^3(v_{1t}+2k_1\alpha_1v_{1x}+(-\alpha_1+\beta_1)u_{1xx})-u_1v_1(-2\beta_1u_{1x}v_{1x}\\&+v_1(v_{1t}+2k_1\alpha_1v_{1x}+(-\alpha_1+\beta_1)u_{1xx}))+v_1^3(u_{1t}+2k_1\alpha_1u_{1x}+(\alpha_1-\beta_1)v_{1xx})\\&+u_1^2(-\beta_1v_{1x}^2+v_1(2v_1(-k_1^2\alpha_1+\omega_1+\lambda_1u_2^2+v_2^2))+u_{1t}+2k1\alpha_1\\&+(\alpha_1-\beta_1)v_{1xx}))=0,\end{aligned} \tag{7}$$

$$v_1(v_{1t}+2k1\alpha_1v_{1x}-\alpha_1u_{1xx})+u_1(u_{1t}+\alpha_1(2k_1u_{1x}+v_{1xx}))=0, \tag{8}$$

$$\begin{aligned}&u_2^4(-k_2^2\alpha_2+\omega_2+\lambda_2(u_1^2+v_1^2))-u_2^3(v_{2t}+2k_2\alpha_2v_{2x}+(-\alpha_2+\beta_2)u_{2xx})\\&-u_2v_2(-2\beta_2u_{2x}v_{2x}+v_2(v_{2t}+2k_2\alpha_2v_{2x}+(-\alpha_2+\beta_2)u_{2xx}))\\&+v_2^2((-k_2^2\alpha_2+\omega_2+\lambda_2(u_1^2+v_1^2))v_2^2-\beta_2u_{2x}^2+v2(u_{2t}+2k_2\alpha_2u_{2x}+(\alpha_2-\beta_2)v_{2xx}))\\&+u_2^2(-\beta_2v_{2x}^2+v_2(2(-k_2^2\alpha_2+\omega_2+\lambda_2(u_1^2+v_1^2))v_2+u_{2t}\\&+2k_2\alpha_2u_{2x}+(\alpha_2-\beta_2)v_{2xx}))=0,\end{aligned} \tag{9}$$

$$\begin{aligned}&u_2^2v_{2(}v_{2t}+2k_2\alpha_2v_{2x}-\alpha_2u_{2xx})+v_2^3(v_{2t}+2k_2\alpha_2v_{2x}-\alpha_2u_{2xx})\\&+u_2v_2^2(u_{2t}+\alpha_2(2k_2u_{2x}+v_{2xx}))+u_2^3(u_{2t}+\alpha_2(2k2u_{2x}+v_{2xx)})=0.\end{aligned} \tag{10}$$

Here, we search for traveling waves solutions of (7)-(10). To this end we put $u_i(x,t)=U_i(z),v_i(x,t)=V_i(z),i=1,2$ and $z=\mu x+\sigma t$. Thus, (7)–(10) reduce, respectively, to

$$\begin{aligned}&U_1^4(-k_1^2\alpha_1+\omega_1+\lambda_1(U_2^2+V_2^2))+U_1^3(-(2k_1\alpha_1\mu+\sigma)V_1'+(\alpha_1-\beta_1)\mu^2U_1'')\\&+U_1V_1(-((2k_1\alpha_1\mu+\sigma)V_1-2\beta_1\mu^2U_1')V_1'+(\alpha_1-\beta_1)\mu V_1U_1'')\\&+V_1^2(V_1(-k_1^2\alpha_1+\omega_1+\lambda_1(U_2^2+V_2^2)-\beta_1\mu^2U_1'^2+V_1((2k_1\alpha_1\mu+\sigma)U_1'\\&+(\alpha_1-\beta_1)\mu^2V_1''))+U_1^2(2V_1^2(-k_1^2\alpha_1+\omega_1+\lambda_1(U_2^2+V_2^2))\\&-\beta_1\mu^2V_1'^2+V_1((2k_1\alpha_1\mu+\sigma)U_1'+(\alpha_1-\beta_1)\mu^2V_1'')=0,\end{aligned} \tag{11}$$

$$V_1((2k_1\alpha_1\mu+\sigma)V_1'-\alpha_1\mu^2U_1'')+U_1((2k_1\alpha_1\mu+\sigma)U_1'+\alpha_1\mu^2V_1'')=0, \tag{12}$$

$$\begin{aligned}&U_2^4(-k_2^2\alpha_2+\omega_2+\lambda_2(U_1^2+V_1^2))+U_2^3(-(\sigma+2k_2\alpha_2\mu)V_2'\\&+(\alpha_2-\beta_2)\mu^2U_2'')+U_2V_2(-((2k_2\alpha_2\mu]+\sigma)V_2-2\beta_2\mu^2U_2')V_2'\\&+(\alpha_2-\beta_2\mu^2V_2U_2'')+V_2^2((-k_2^2\alpha_2+\omega_2+\lambda_2(U_1^2+V_1^2)V_2^2\\&-\beta_2\mu^2U_2'^2+V_2((2k_2\alpha_2\mu+\sigma)U_2'+(\alpha_2-\beta_2)\mu^2V_2''))+U_2^2(2(-k_2^2\alpha_2+\omega_2+\\&\lambda_2(U_1^2+V_1^2))V_2^2-\beta_2\mu^2V_2'^2+V_2((2k_2\alpha_2\mu+\sigma)U_2'+(\alpha_2-\beta_2)\mu^2V_2''))=0,\end{aligned} \tag{13}$$

$$\begin{aligned}&U_2^2V_2((2k_2\alpha_2\mu+\sigma V_2'-\alpha_2\mu^2U_2'')+V_2^3((2k_2\alpha_2\mu+\sigma)V_2'-\alpha_2\mu^2U_2'')\\&+U_2V_2^2((2k_2\alpha_2\mu+\sigma)U_2'+\alpha_2\mu^2])+U_2^3((2k_2\alpha_2\mu+\sigma)U_2'+\alpha_2\mu^2V_2'')=0.\end{aligned} \tag{14}$$

Here,the exact solutions of (11)–(14) (or (7)–(10)) are found by using the unified method [39–42]. By this method solutions of a NLPDE are written in a polynomial or a rational functions (PF or RF) in auxiliary functions, with appropriate auxiliary equations.

PF. Solutions of (11)–(14)

The solutions are represented in polynomial forms in an auxiliary function that satisfies an auxiliary equation,

$$\begin{aligned}&U_1(z)=\sum_{i=0}^{n_1}a_i\,g^i(z),\ \ V_1(z)=\sum_{i=0}^{n_2}b_i\,g^i(z),\\&U_2(z)=\sum_{i=0}^{m_1}h_i\,g^i(z),\ \ V_2(z)=\sum_{i=0}^{m_2}p_i\,g^i(z),\\&g'(z)^p=\sum_{i=0}^{pk}c_i\,g^i(z),\ p=1,2,\end{aligned} \tag{15}$$

where n_i,m_i and k are integers. First we consider the case $p=1$. Here,

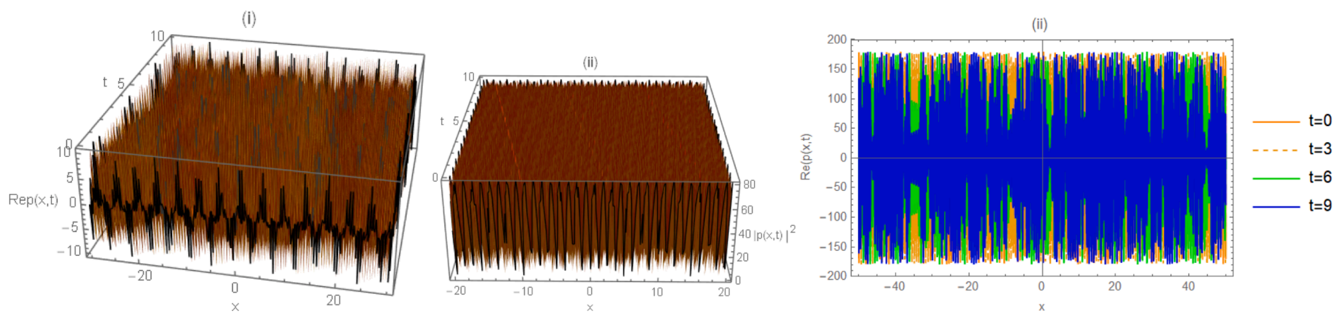

Fig. 1. Figs. 1(i)–(iii) In (i) 3D plot to $Rep(x,t)$ is displayed against x and t. In (ii) 3D plot to $|p(x,t)|$ against x and t. In (iii) $Rep(x,t)$ is displayed against x for different values of t. When $a_0 = 2, a_1 = 1.5, h_1 = 0.8, \lambda_1 1.5, \alpha_1 = 5.5, \beta_1 = 0.5, \sigma = 5$, $\mu = 6, k_1 = 1.5, \lambda_2 = -0.5, \alpha_2 = 5.8, k_2 = 3, \beta_2 = 6, m = 1.5, n = 1.3$.

the objective is to finding n_i, m_i and k. To this end, balance of the nonlinear and higher order derivative terms are invoked. Which determines $n_i = n_i(\mathrm{k})$, $m_i = m_i(\mathrm{k})$, which is called the balance condition. These conditions read $n_i = m_i = k-1, i = 1,2$. To determine the value of k, we need to evaluate: (i) The number of equations that result from substituting (15) into. (11)–(14) and setting the coefficients o $g^j(z), j = 0, 1, 2$ equal to zero (say$r(k)$). (ii) The number of arbitrary paymasters $\{a_j, b_j, h_i, p_i, c_j\}$in (15) (says$(k)$), and the highest order derivative (say m). When (11)–(14) are integrable, we have $r(k) - s(k) \leqslant m$, which leads to get k. This last condition is the consistency condition and, in the present case, it reads $1 \leqslant k \leq 3$. By the same the case $p = 2$ is dealt with.

Elliptic pulses: $p = 2$ and $k = 2$.

In this case, (15) becomes

$$\begin{gathered} U_1(z) = a_1 g(z) + a_0, \quad V_1(z) = b_1 g(z) + b_0, \\ U_2(z) = h_1 g(z) + h_0, \quad V_2(z) = p_1 g(z) + p_0 \\ g^{'}(z) = \sqrt{c_4 g(z)^4 + c_2 g(z)^2 + c_0}. \end{gathered} \tag{16}$$

By substituting (16) into (11)–(14), and for the real and imaginary parts to be linearly dependent, we take $b_0 = a_0 b_1 / a_1$and $p_0 = h_0 p_1 / h_1$. By setting the coefficients of $g(z)^j, j = 0, 1, \ldots$, equal to zero, we get

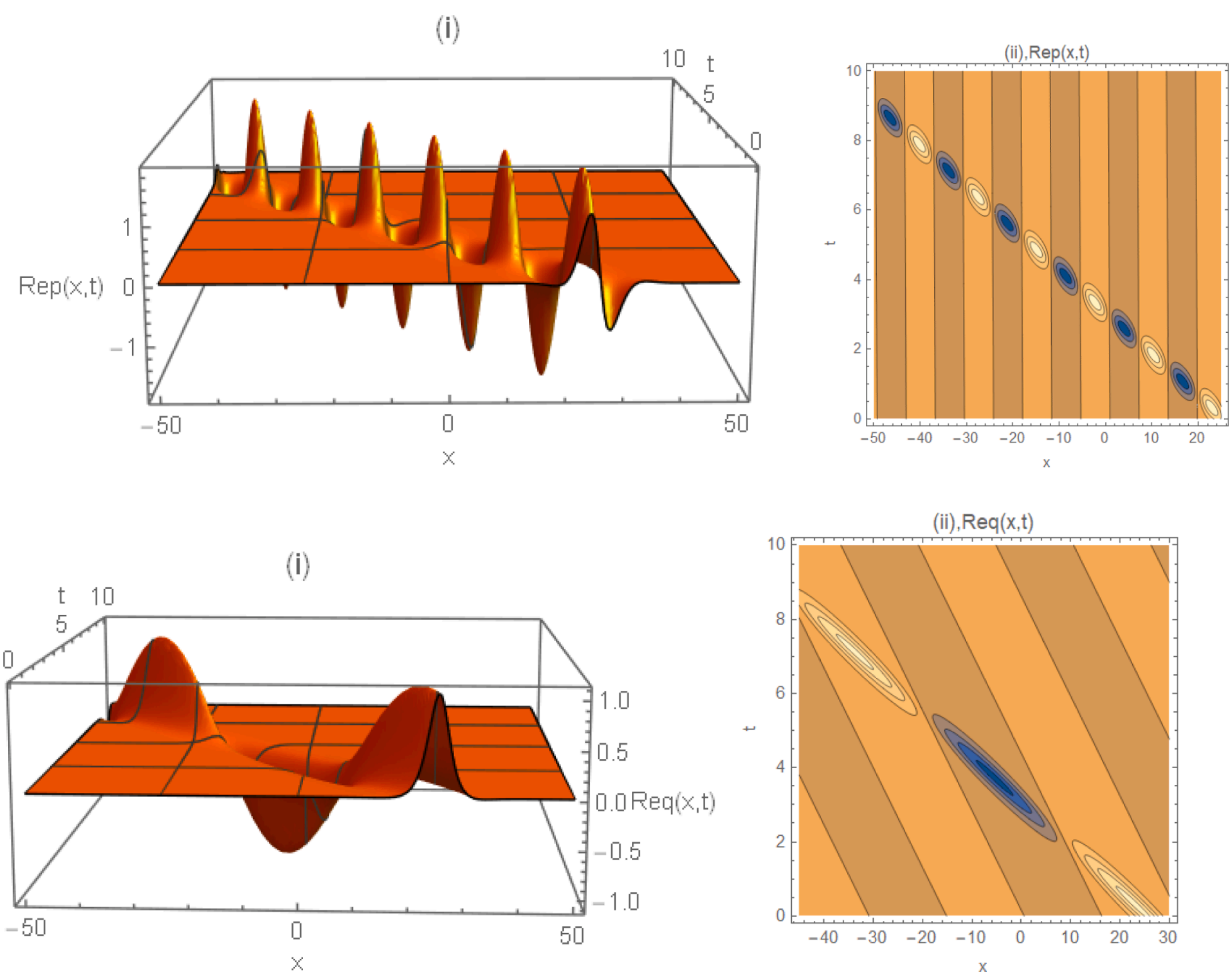

Fig. 2. Fig. 2(i), (ii) for the first and second modes respectively. The 3D- and contour plots are shown in (i) and (ii) respectively.When $B_0 = -20, a_1 = 5, h_1 = 0.7$, $\lambda_1 = 1.5, \alpha_1 = 3.5, \beta_1 = 0.5, \sigma = 5, = 0.6, k_1 = 0.5, \lambda_2 = 0.5, \alpha_2 = 3.8, \beta_2 = 0.8, k_2 := 0.2, a = 0.7, c = 1.3, b := 4$.

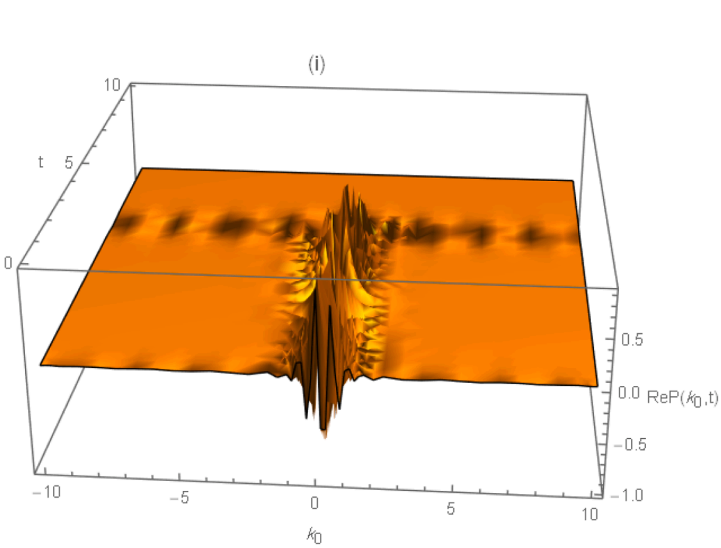

Fig. 3. Fig. 3(i) and (ii). The 3D and contour plots are displayed against x and t for the same caption as in Figs. 2.

$$\omega_1 = \frac{h_1^2 k_1^2 \alpha_1 - (h_1^2 + p_1^2) h_0^2 \lambda_1}{h_1^2}, \quad = -\frac{a_0 h_1}{2a_1}, \quad c_2 = 0, \tag{17}$$

$$p_1 = \pm\frac{1}{\sqrt{\lambda_1}}\sqrt{-h_1^2\lambda_1 - 2c_4\alpha_1\mu^2 + 2c_4\beta_1\mu^2}, \quad ao := \frac{a_1\sqrt{c_2}}{\sqrt{-2c_4}},$$

$$\omega_2 = -(\frac{k_2^2((a_1^2 + b_1^2)\lambda_2 - 2c_4\beta_2\mu^2)}{2c_4\mu^2}, \quad b_1 = \pm\frac{\sqrt{-a_1^2\lambda_2 + 2c_4(-\alpha_2 + \beta_2)\mu^2}}{\sqrt{\lambda_2}}. \tag{18}$$

The solution of the auxiliary equation, in (16), is

$$c_4 = -m^2, \; c_0 = n^2, \quad g(z) = \pm\frac{n\, sn(\sqrt{2}nmz, \frac{1}{\sqrt{2}})}{m\sqrt{2 - sn(\sqrt{2}nmz, \frac{1}{\sqrt{2}})^2}}, \; z = \mu x + \sigma t. \tag{19}$$

Finally the solutions of (11)–(14) are

$$u_1(x,t) = \pm\frac{a_1\, n\, sn(\sqrt{2}nmz, \frac{1}{\sqrt{2}})}{m\sqrt{2 - sn(\sqrt{2}nmz, \frac{1}{\sqrt{2}})^2}}, \quad v_1(x,t) = \pm\frac{\sqrt{-a_1^2\lambda_2 + 2c_4(-\alpha_2 + \beta_2)\mu^2}}{a_1\sqrt{\lambda_2}} u(x,t),$$

$$u_2(x,t) = \frac{h_1}{a_1} u_1(x,t), \quad v_2(x,t) = \pm\frac{1}{a_1\sqrt{\lambda_1}}\sqrt{-h_1^2\lambda_1 - 2c_4\alpha_1\mu^2 + 2c_4\beta_1\mu^2 u_1(x,t)}. \tag{20}$$

It is worthy to mention that the presence of $\pm$ signs reflect a fact that each solution $u_i(x,t)$ and $v_i(x,t)$, $i = 1,2$ can be expressed by two solutions which may be called right and left solutions, They correspond to the upper and lower signs respectively. Here, we confine our selves to consider the upper sign.

The results in (20) are represented in Figs. 1(i), (ii) and (iii) for the first mode.

Fig. 1(i) shows complex chirped while (ii) shows Mixed M-W-shaped pulses. Fig. 1(iii) shows chaotic waves.

The critical values of β_i, $i = 1,2$ that distinguish the polarization of the first and second modes are given in the following

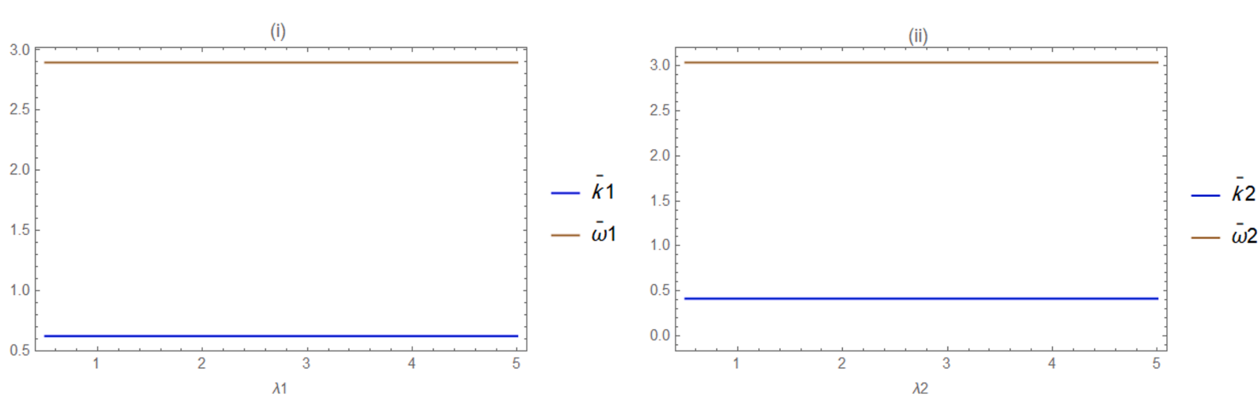

Fig. 4. Fig. 4(i) and (ii) are displayed for the same caption as in Figs. 2(i) and (ii).

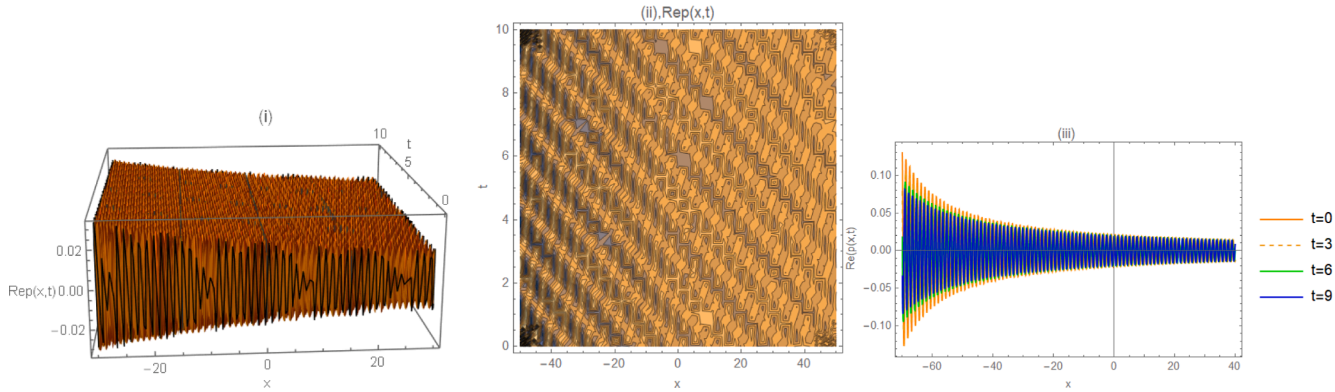

Fig. 5. Figs. 5(i)–(iii). The 3D and contour plots are shown in (i) and (ii). In (iii0 the solutions in (30), for the first mode,are displayed against x for different values of t.

$$\lambda_1<0,\ \beta_1>\frac{-h_1^2\lambda_1+2m^2\alpha_1\mu^2}{2m^2\mu^2}, or\quad \lambda_1>0,\quad \beta_1<\frac{-h_1^2\lambda_1+2m^2\alpha_1\mu^2}{2m^2\mu^2},$$
$$\lambda_2<0,\ \beta_2>\frac{-a_1^2\lambda_2+2m^2\alpha_2\mu^2}{2m^2\mu^2}, or\quad \lambda_2>0,\quad \beta_2<\frac{-a_1^2\lambda_2+2m^2\alpha_2\mu^2}{2m^2\mu^2}. \tag{21}$$

Lumps: $p=2$ *and* $k=2$

In this case we consider the solutions given in (16), but the auxiliary equation is

$$g'(z)=cg(z)\sqrt{a^2-b^2g(z)^2}. \tag{22}$$

By using (16) and (22) in (11)–(14), we have

$$a_0=0,\ h_0=0,\ \omega_1=k_1^2\alpha_1+a^2c^2(-\alpha_1+\beta_1)\mu^2,$$
$$p_1=\pm\frac{\sqrt{-h_1^2\lambda_1-2b^2c^2(-\alpha_1+\beta_1)\mu^2}}{\sqrt{\lambda_1}}, \tag{23}$$

$$b_1=\pm\frac{\sqrt{-a_1^2\lambda_2+2b^2c^2\mu^2(\alpha_2-\beta_2)}}{\sqrt{\lambda_2}},\quad \omega_2=k_2^2\alpha_2-a^2c^2(\alpha_2-\beta_2)\mu^2. \tag{24}$$

Finally the solutions are, where the upper sign is taken,

$$u_1(x,t)=\frac{(aa_1 sech(a(B_0+cz))/}{b},\ v_1(x,t)=\frac{\sqrt{-a_1^2\lambda_2+2b^2c^2\mu^2(\alpha_2-\beta_2)}}{a_1\sqrt{\lambda_2}}u_1(x,t),$$
$$u_2(x,t)=\frac{h_1}{a_1}u_1(x,t),\ v_2(x,t)=\frac{1}{a_1\sqrt{\lambda_1}}\sqrt{-h_1^2\lambda_1-2b^2c^2(-\alpha_1+\beta_1)\mu^2}u_1(x,t). \tag{25}$$

The results for the first and second modes are shown in Figs. 2, (i) and (ii) respectively.

Figs. 2(i) shows multiple lumps while (ii) shows wavy soliton.

The characteristics of the pulses configurations are demonstrated in what it follows. We mention that the Eqs. (3)–(5) are used. The spectrum for the first mode is shown in Figs. 3 (i) and (ii).

Figs. 3 show chaotic optical pulses near $k_0=0$. Otherwise, it shows Random optical pulses.

The frequencies and wave lengths are shown in Figs. 4(i) and (ii).

Here, both $\overline{\omega_i}$ and $\overline{k_i}, i=1,2$ are constant for any parameters in the solution (25).

In this case the polarization of the two modes is determined whenever the following equations hold

$$\lambda_1<0,\ \beta_1>\frac{-h_1^2\lambda_1+2b^2c^2\alpha_1\mu^2}{2b^2c^2\mu^2}\ or\,\lambda_1>0,\ \beta_1<\frac{-h_1^2\lambda_1+2b^2c^2\alpha_1\mu^2}{2b^2c^2\mu^2},$$
$$\lambda_2<0,\ \beta_2>\frac{-a_1^2\lambda_2+2b^2c^2\alpha_1\mu^2}{2b^2c^2\mu^2}\ or\,\lambda_2>0,\ \beta_2<\frac{-a_1^2\lambda_2+2b^2c^2\alpha_1\mu^2}{2b^2c^2\mu^2}. \tag{26}$$

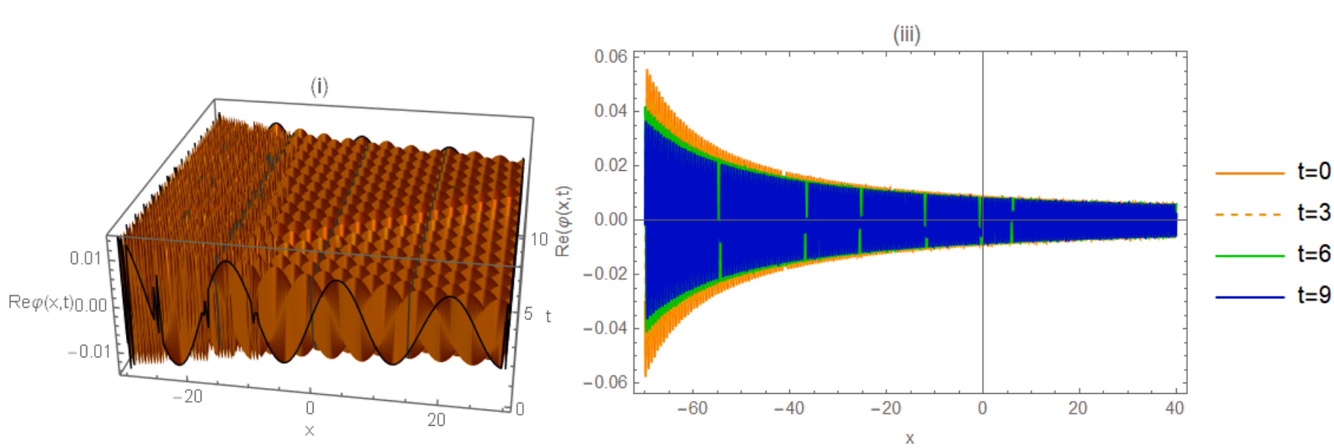

Fig. 6. Figs. 6(i) and (ii). The 3D plot and the variation against x for different values of time for the second mode are shown in (i) and (ii) respectively. The same caption as in Figs. 5(i) and (ii) are used..

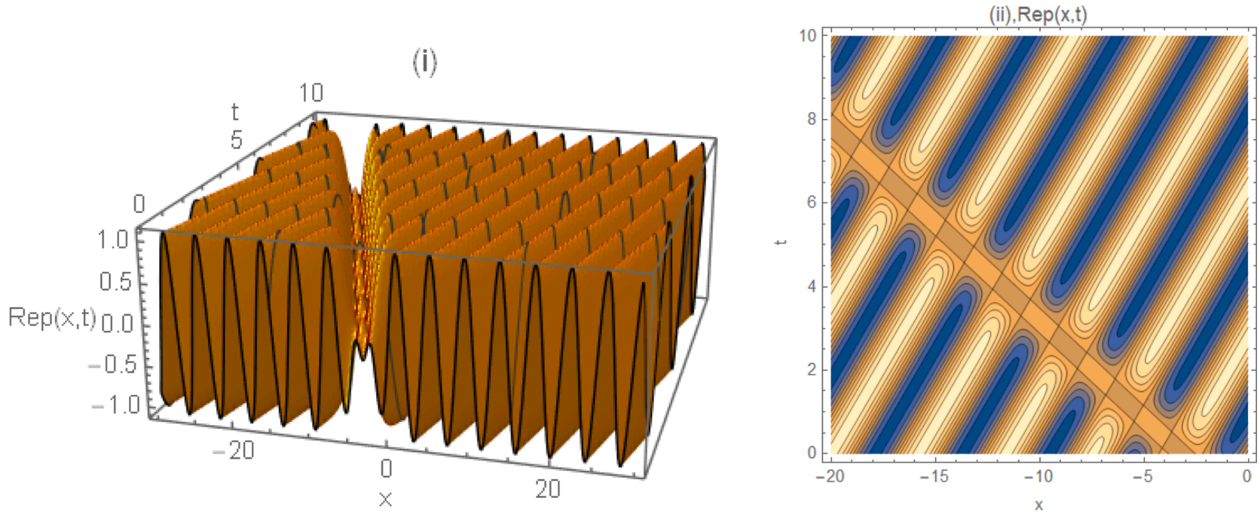

Fig. 7. Figs. 7(i), and (ii). The 3D and contour plots are displayed $Rep(x,t)$ are displayed when $a_0 = 0.2, s_1 = 1.5, B_0 = 4, c = 1.8, a_1 = 0.5, h_1 = 0.8, \alpha_2 = 1.5, \lambda_1 = 0.09, \lambda_2 = -1.5, \mu = 0.7, \sigma = 1.5, a = 1.1, = 4, c = 1.8, h_0 = 3.1, s_0 = 1.3, \beta_2 = -0.4, \beta_1 = 3.7$.

Solitary: when $p = 1$ and $k = 2$

In this case we consider the solutions given in (16), but the auxiliary equation is

$$g'(z) = c_2 g(z)^2 + c_1 g(z) + c_0. \tag{27}$$

By inserting (16) and (27) in (11)–(14), we have

$$\omega_1 = k_1^2\alpha_1 - \frac{h_0^2(h_1^2+p_1^2)h_0^2\lambda_1}{b_1^2} + \frac{a_1c_1c_0(-\alpha_1+\beta_1)\mu^2}{a_0}, \quad c_0 = \frac{a_0(a_1c_1 - a_0c2))}{a_{2\,1}},$$

$$p_1 = \frac{\sqrt{-h_1^2\lambda_1 + 2c_2^2(-\alpha_1+\beta_1)\mu^2}}{\sqrt{\lambda_\cdot}}, \quad h_0 = \frac{h_1}{4a_1c_2}(-2a_0c_2 + 3c_1a_1). \tag{28}$$

$$b_1 = \frac{\sqrt{2c_2^2(-\alpha_2+\beta_2)\mu^2a_1^2\lambda_2}}{\sqrt{\lambda_2}}, \quad c_2 = \frac{a_1c_1}{2a_0}, \quad \omega_2 = k_2^2\alpha_2. \tag{29}$$

Finally, we have

$$g(z) = -\frac{a_0(2 + c_2z + 2a_1a_0A_0)}{a_1(c_1z + 2a_1a_0A_0)}, \quad u_1(x,t) = -\frac{2a_0}{2a_1a_0A_0 + c_1z},$$

$$v_1(x,t) = -\frac{\sqrt{2}a_0\sqrt{-2a_0^2\lambda_2 + c_1^2(-\alpha_2+\beta_2)\mu^2}}{(2a_1a_0A_0 + c_1z)\sqrt{\lambda_2}}, \quad u_2(x,t) = h_1u_1(x,t), \tag{30}$$

$$v_2(x,t) = -\frac{\sqrt{-4h_1\lambda_1 1a_0 + 2a_1c_1(-\alpha_1+\beta_1)\mu^2}}{(2a_1a_0A_0 + c_1z)\sqrt{\lambda_1}} uz = \mu x + \sigma t.$$

The results in (30) for the first and second modes are displayed in Figs. 5(i)–(iii) and 6(i) and (ii).

When $A_0 = 100, a_0 = 2, a_1 = 5, c_1 = 4, h_1 = 0.8, \lambda_1 = -0.5, \alpha_1 = 1.5, \beta_1 = 3, \sigma = 5, \mu = 6; k_1 = 5, \lambda_2 = 2.5, \alpha_2 = 0.8, \beta_2 = 1.8, k2 := 10$.

Figs. 5 (i) shows soliton cascade, (ii) shows random optical lattice and (iii) show self modulation waves.

The behavior of the solutions for second mode are shown in Figs. 6(i) and (ii).

In this figure, the behavior of the solution is mainly the same as in Figs. 5.

RF solutions of (11)–(14)

When $p = 1$ and $k = 1$

Here, we find rational solutions in the form

$$U_1(z) = \frac{a_1g(z) + a_0}{s_1g(z) + s_0}, \quad V_1(z) = \frac{b_1g(z) + b_0}{s_1g(z) + s_0},$$
$$U_2(z) = \frac{h_1g(z) + h_0}{s_1g(z) + s_0}, \quad V_2(z) = \frac{p_1g(z) + p_0}{s_1g(z) + s_0}. \tag{31}$$
$$g'(z) = c_1g(z) + c_0$$

For linearly dependent solutions, we take$b_0 = \frac{a_0b_1}{a_1}$, $p_0 = \frac{h_0p_1}{h_1}$. By inserting (31) into (11)–(14), we get

$$h_0 = \frac{h_1(a_0c_1^2s_1^3(-\alpha_1+\beta_1)\mu^2 + 2a_1s_0\lambda_1(h_1^2+p_1^2 - c_1^2s_1^2(-\alpha_1+\beta_1)\mu^2))}{2a_1(h_1^2+p_1^2)s_1\lambda_1},$$

$$c_0 = \frac{1}{12a_1(h_1^2+p_1^2)s_1\lambda_1}c_1(8a_1s_0\lambda_1(h_1^2+p_1^2) + c_1^2s_1^2(\alpha_1-\beta_1)\mu^2) + 4a_0s_1\lambda_1(h_1^2+p_1^2) + c_1^2s_1^2(-\alpha_1+\beta_1)\mu^2), \tag{32}$$

$$\omega_2 = k_1^2\alpha_1 - \frac{(h_1^2+p_1^2)\lambda_1}{s_1^2}, \quad p_1 = \frac{1}{\sqrt{2\lambda_1}}\sqrt{-2h_1^2\lambda_1 + c_1^2s_1^2(-\alpha_1+\beta_1)\mu^2},$$

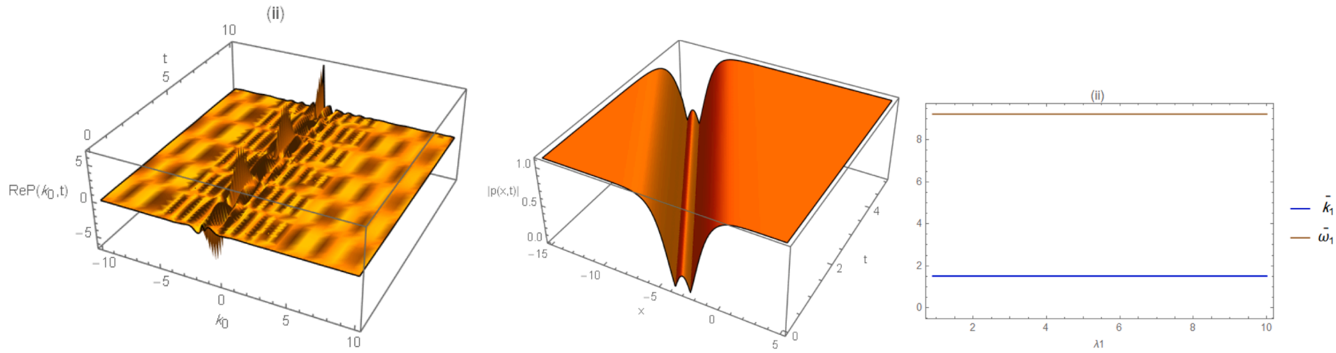

Fig. 8. Figs. 8(i), (ii) and (iii). The spectrum, intensity frequency and wave number are shown in (i), (ii) and (iii) respectively for the same caption as in Figs. 7(i), (ii).

$$\omega_2 = k_2^2\alpha_2 - \frac{(a_1^2+b_1^2)\lambda_2}{s_1^2}, \quad b_1 = \frac{1}{\sqrt{2\lambda_2}}\sqrt{-2a_1^2\lambda_2 c_1^2 s_1^2(-\alpha_2+\beta_2)\mu^2} \tag{33}$$

Finally the solutions are

$$u_1(x,t) = \frac{a_1(a_0 s_1 + 2a_1 A_0 e^{c_1 z} s_1 - a_1 s_0)}{s_1(-a_0 s_1 + a_1(2A_0 e^{c_1 z} s_1 + s_0))}, \quad v_1(x,t) = \frac{b_1}{a_1}u_1(x,t),$$
$$u_2(x,t) = -\frac{h_1}{a_1}u_1(x,t), \quad v_2(x,t) = \frac{p_1}{a_1}u_1(x,t). \tag{34}$$

When $p = 1$ and $k = 2$

In this case we use (31) but the auxiliary equation is taken

$$g'(z) := c_2\, g(z)^2 + c_1\, g(z) + c_0, \tag{35}$$

g[z]g[z]and we take $b_0 = \frac{a_0 b_1}{a_1}$, *and* $p_0 = \frac{h_0 p_1}{h_1}$. By substituting from (31) and (35) into (11)–(14), we get

$$\omega_1 = k_1^2\beta_1 - \frac{(a_0h_1 - a_1h_0)^2(h_1^2+p_1^2)\lambda_1}{9\,h\,s_1^2} - \frac{2a_1^2h_1^2(5a_0h_1 + a_1ho)^2k_1^2(h_1^2+p_1^2)\lambda_1}{9c_2^2h^2s_1^2\mu^2},$$
$$h = (3a_0h_1 + a_1h_0)^2, \quad c_0 = \frac{a_0c_2(-a_0^2h_1^2 + 5a_1a_0h_1h_0 + 2a_1^2h_0^2)}{a_1^2h_1(5a_0h_1 + a_1h_0)},$$
$$c_1 = \frac{4a_0^2c_2h_1^2 + 6a_1a_0c_2h_1h_0 + 2a_1^2c_2h_0^2}{a_1h_1(5a_0h_1 + a_1h_0)}, \quad p = \frac{\sqrt{K}}{\sqrt{2}\sqrt{[-a_1^2h_1^2(5a_0h_1 + a_1h_0)^2\lambda_1}}, \tag{36}$$
$$K = \lambda_1(50a_0^2a_0^2h_1^6 + 20a_1^3a_0h_1^5h_0 + 2a_1^4h_1^4h_0^2) + 9c_2^2(3a_0h_1 + a_1h_0)^4 s_1^2\alpha_1\mu^2 - 9c_2^2(3a_0h_1 + a_1h_0)^4 s_1^2\beta_1\mu^2,$$

$$\omega_2 = -\frac{k_2^2(a_1^4\lambda_2 + a_1^2b_1^2\lambda_2 - 32a_0^2c_2^2s_1^2\beta_2\mu^2)}{32a_0^2c_2^2s_1^2\mu^2}, \quad h_0 = \frac{a_0h_1}{a_1},$$
$$b_1 = \frac{1}{\sqrt{\lambda_2}}\sqrt{-a_1^4\lambda_2 - 32a_0^2c_2^2\widehat{2}s_1^2\alpha_2\mu^2 + 32a_0^2c_2^2s_1^2\beta_2\mu^2}. \tag{37}$$

Finally the solutions are

$$u_1(x,t) = \frac{a_1^2}{(a_1s_1 + 4a_1^2a_0A_0s_1 + 4a_0c_2s_1z)}, \quad v_1(x,t) = \frac{b_1}{a_1}u_1(x,t),$$
$$u_2(x,t) = -\frac{h_1}{a_1}u_1(x,t), \quad v_2(x,t) = \frac{p_1}{a_1}u_1(x,t), \; z = \mu x + \sigma t. \tag{38}$$

When $p = 2$ and $k = 2$

Here, we use (31) together with the auxiliary equation

$$g'(z) = cg(z)\sqrt{a^2 - b^2g(z)^2}. \tag{39}$$

By using (31) and (39), we have

$$\omega_1 = k_1^2\alpha_1 - \frac{h_0^2(h_1^2+p_1^2)\lambda_1}{h_1^2s_0^2}, \quad b = \frac{a\sqrt{3h_0^2s_1^2 + 4h_1h_0s_1s_0 + h_1^2s_0^2}}{2\sqrt{2}h_0s_0},$$
$$a_1 = \frac{ao}{a^2c^2h_1^2s_0^3(\alpha_1-\beta_1)\mu^2}(\lambda_1(2h_0^2p_1^2s_1 - 2h_1^3h_0s_0 - 2h_1h_0p_1^2s_0) + h_1^2s_1(2h_0^2\lambda_1 + a^2c^2s_0^2(\alpha_1-\beta_1)\mu^2)), \tag{40}$$
$$p_1 = \frac{h_1\sqrt{K}}{2\sqrt{h_0^2(h_0s_1 - h_1s_0)\lambda_1}}, \quad K = (-4h_0^3s_1 + 4h1h_0^2s_0)\lambda_1 + (-\alpha_1+\beta_1)\mu^2(5a^2c^2h_0s_1s_0^2 + a^2c^2h_1s_0^3),$$

$$\omega_2 = k_2\widehat{2}\alpha_2 - \frac{(b_1^2 s_0^2 - a_0^2 s_1^2)\lambda_2}{s_1^2 s_0^2}, \quad h_1 = -\frac{h_0 s_1}{s_0},$$
$$b_1 = \frac{s_1}{\sqrt{2}s_0}\sqrt{-2a_0^2 + \frac{a^2c^2s_0^2(-\alpha_2+\beta_2)\mu^2}{\lambda_2}}. \tag{41}$$

The solutions of (11)–(14) are

$$u_1(x,t) = \frac{a_0(bs_0 cosh(a(B_0+cz)) - as_1)}{s_0(as_1 + bs_0 cosh(a(B_0+cz)))}, \quad v_1(x,t) = \frac{b_1}{a_0}u_1(x,t)$$
$$u_2(x,t) = \frac{h_1}{a_0}u_1(x,t), \quad v_2(x,t) = \frac{p_1}{a_0}u_1(x,t). \tag{42}$$

The results (41) and (42) are used to display $Rep(x,t)$ in Figs. 7(i) and (ii).

Figs. 7(i) and (ii) show tunable conoidal pulses.This result is novel

We mention that when displaying $Req(x,t)$, we found that the figures show mainly the same behavior, apart from the numerical values of $Rep(x,t)$ and $Req(x,t)$. So, they will not produced here.

The characteristic of pulses, spectrum, frequency wave length and intensity are shown for the two modes Are shown in Figs. 8(i)–(iii).

Fig. 8(i) shows lumps supported by periodic waves, while (ii) shows W-shaped with double kinks.

The same figures are displayed for the second mode.The same behaviors as in Fig. 8(i)–(iii) hold, but with different numerical values and they will not shown here.

Conclusions and future work

Here, the two-mode resonant nonlinear Schrodinger equations are considered. A new transformation that allows to inspect the waves resulting from soliton- periodic wave collision is invoked. Exact solutions of the model equations are found by using the unified method. A class of polynomial and rational solutions have been obtained. It is observed that there is no rogue (or sharp) waves formation, thus collision is elastic. It is shown that the pulses propagation occurs in different geometric structures. Self-phase optical pulses modulation, soliton-cascade, multi-lumps, M-W-shaped, complex chirped and tunable conoidal pulses. It is found that the pulse- polarization, self-focusing or self-defocusing, depends basically on the coefficient of the quantum potential. Further the spectrum content is investigated. It shows mixed lattice and Chaotic spectrum are observed. For future work we shall investigate the pulses configuration in a medium in two-mode chiral nonlinear schrodinger equation.

Funding

C. Park was supported by Basic Science Research Program through the National Research Foundation of Korea funded by the Ministry of Education, Science and Technology (NRF-2017R1D1A1B04032937).

CRediT authorship contribution statement

H.I. Abdel-Gawad: Formal analysis, Methodology, Project administration, Resources, Writing - original draft. **Choonkil Park:** Funding acquisition, Methodology, Resources, Software, Supervision, Validation, Writing - original draft.

Declaration of Competing Interest

The authors declare that they have no known competing financial interests or personal relationships that could have appeared to influence the work reported in this paper.

Acknowledgment

The author would like to thank the reviewers for their pertinent comments that led to improving the presentation of the paper.

References

[1] Serkin VN, Hasegawa A. Novel soliton solutions of the nonlinear Schrödinger equation Model. Phys Rev Lett 2000;85:21.
[2] Tantawy M, Abdel-Gawas HI. On multi-geometric structures optical waves propagation in self-phase modulation medium: Sasa-Satsuma equation. Eur Phys J Plus 2020;135:928.
[3] Abdel-Gawad HI. Solutions of the generalized transient stimulated raman scattering equation. optical pulses compression. Optik 2021. https://doi.org/10.1016/j.ijleo.2021.166314.
[4] Ablowitz M, Musslimani ZH. Integrable nonlocal nonlinear Schrödinger equation. Phys Rev Lett 2013;110:064105.
[5] Guo B, Ling L, Liu QP. Nonlinear Schrödinger equation: Generalized Darboux transformation and rogue wave solutions. Phys Rev E 2012;85:026607.
[6] d'Avenia P. Non-radially symmetric solutions of nonlinear Schrödinger equation coupled with Maxwell equations. Adv Nonlinear Stud 2016;2:2.
[7] Carr LD, Clark Charles W, Reinhardt WP. Stationary solutions of the one-dimensional nonlinear Schrödinger equation. II. Case of attractive nonlinearity. Phys Rev A 2000;62:063611.
[8] Alfano RR, Shapiro SL. Observation of self-phase modulation and small-scale filaments in crystals and glasses. Phys Rev Lett 1970;24:592.
[9] Anderson D, Lisak M. Nonlinear asymmetric self-phase modulation and self-steepening of pulses in long optical wave guides. Phys Rev A 1983;27:1393.
[10] Perry MD, Ditmire T, Stuart BC. Self-phase modulation in chirped-pulse amplification. Opt Lett 1994;19:2149–52.
[11] Lee JH, Pashaev OK, ROGERS C, SCHIEF K. The resonant nonlinear Schrödinger equation in cold plasma physics. Application of Bäcklund–Darboux transformations and superposition principles. J Plasma Phys 73(2);2007:257–272.
[12] Tzoar N, Jain M. Self-phase modulation in long-geometry optical wave guides. Phys Rev A 1981;23:1266.
[13] Abdel-Gawad HI, Tantawy M, Inc M, Yusuf A. Construction of rogue waves and conservation laws of the complex coupled Kadomtsev- Petviashvili equation., Int J Mod Phys B 2020:2050115–2050134.
[14] Pashaev OK, Lee JH. Resonance solitons as black holes in Madelung fluid. Mod Phys Lett A 2002;17(24):1601–19.
[15] Inc M, Aliyu AI, Yusuf A, Baleanu D. Optical solitons to the resonance nonlinear Schrödinger equation by Sine-Gordon equation method. Superlatt Microstruct 2018;113:541–9.
[16] Lee JH, Pashaev OK, Rogers C, Schief WK. The resonant nonlinear Schrödinger equation in cold plasma physics: application of Bäcklund-Darboux transformations and superposition principles. J Plasma Phys 2006;73(2):257–72.
[17] Eslami M, Mirzazadeh M, Biswas A. Soliton solutions of the resonant nonlinear Schrödinger's equation in optical fibers with time-dependent coefficients by simplest equation approach. J Mod Opt 2013;60(19):1627–36.
[18] Hosseini K, Manafian J, Samadani F, Foroutan M, Mirzazadeh M, Zhou Q. Resonant optical solitons with perturbation terms and fractional temporal evolution using improved tan(/2)-expansion method and exp function approach. Optik 158;2018: 933–939.
[19] Kumar D, Park C, Tamanna N, Paul GC, Osman MS. Dynamics of two-mode Sawada-Kotera equation: Mathematical and graphical analysis of its dual-wave solutions. Res Phys 2020;19:103581.
[20] Ferdous F, Hafez MG, Biswas A, Ekici M, Zhou Q, Alfiras M, Moshokoa SP et al. Oblique resonant optical solitons with Kerr and parabolic law nonlinearities and fractional temporal evolution by generalized exp -expansion. Optik 178:2019; 439–448.
[21] Inc M, Yusuf A, Aliyu AI, Baleanu D. Optical soliton solutions for the higher-order dispersive cubic-quintic nonlinear Schrödinger equation. Superlatt Microstruct 2017;112:164–79.
[22] Abdel-Gawad HI, Tantawy M, Inc M, Yusuf A. On multi-fusion solitons induced by inelastic collision for quasi-periodic propagation with nonlinear refractive index and stability analysis. Mod Phys Lett B 2018;32:1–8.
[23] Lee J-H, Lin C-K, Pashev OK. Shock waves, chiral solitons and semi-classical limit of one-dimensional anyons. Chaos, Solitons Fract 2004;19(1):109–28.
[24] Akhmanov A, Sukhorukov AP, Khokhlov RV. Self-focusing and diffraction of light in a nonlinear medium. Sov Phys Uspékhi 1968;93:609–36.
[25] Biswas A, Zhou Q, Moshokoaa SP, Triki H, Belic M, Rubayyi M, Alqahtan T. Resonant 1-soliton solution in anti-cubic nonlinear medium with perturbations. Optik 2017;145:14–7.
[26] Meradji S, Triki H, Zhouc Q, Biswas A, Ekici M, Liu, Chirped self-similar cnoidal waves and similaritons in an inhomogeneous optical medium with resonant nonlinearity. Chaos, Solitons Fract 141;2020:110441.
[27] Pathaniaa S, Goyalb A, Rajuc TS, Kumar CN. Chirped nonlinear resonant states in femtosecond fiber optics. Optik 2021;227:166094.
[28] Seadawy AR, Ali MN, Husnin SM, Noor S. Conservation laws and optical solutions of the resonant nonlinear Schrödinger's equation with parabolic nonlinearity. Optik 2021;225:165762.
[29] Kudryashov NA. Optical solitons of the resonant nonlinear Schrödinger equation with arbitrary index. Optik 2021;235:166626.

[30] Eslami M, Mirzazadeh M, Biswas A. Soliton solutions of the resonant nonlinear Schrödinger's equation in optical fibers with time-dependent coefficients by simplest equation approach. J Mod Opt 2013;60(19).

[31] Trikia H, Hayat T, Aldossary OM, Biswas A. Bright and dark solitons for the resonant nonlinear Schrödinger's equation with time-dependent coefficients. Opt Laser Tech 2012;44(7):2223–31.

[32] Awan AU, Rehman HU, Tahir M, Ramzan M. Optical soliton solutions for resonant Schrödinger equation with anti-cubic nonlinearity. Optik 2021;227:165496.

[33] Das A, Jash S, Paul S, Mondala YA, Das A. Optical chirped soliton structures in generalized derivative resonant nonlinear Schrödinger equation and modulational stability analysis,. Optik 226;2021:165701.

[34] Das A, Saha A., Ghosh N. Dynamical behavior of the optical traveling pulses for the resonant nonlinear Schrödinger equation with external periodic force. Int J Mod Phys B 34(27);2020:2050255.

[35] El-Nabulsi RA. On nonlocal complexified Schrödinger equation and emergence of discrete quantum mechanics. Quantum Stud: Math Found 2016;3:327–35.

[36] Biswas A, Ullahb MZ, Zhou Q, Moshokoa SP, HouriaTriki H, Belic M. Resonant optical solitons with quadratic-cubic nonlinearity by semi-inverse variational principle. Optik 2017;145:18–21.

[37] Biswas A, Zhou Q, Triki H, Ullah MZ, Mir Asma M, Seithuti P Moshokoa SP, Belic M. Resonant optical solitons with parabolic and dual-power laws by semi-inverse variational principle. J Mod Opt 65(2);2018:179–184.

[38] Hadi Rezazadeh H, Tariq KU, Sabi'u J, Bekir A. Abundant traveling wave solutions to the resonant nonlinear Schrödinger's equation with variable coefficients. Mod Phys Lett B 34(12);2020:2050118.

[39] Abdel-Gawad HI. Solutions of the generalized transient stimulated Raman scattering equation.Optical pulses compression. Optik 2021;230:16631.

[40] Abdel-Gawad HI, Dumitru Baleanu D, Abdel-Gawad AH. Unification of the different fractional time derivatives: An application to the epidemic-antivirus dynamical system in computer networks. Chaos, Solitons Fract 2021;142:110416.

[41] Srivastava HM, Abdel-Gawas HI, Saad KM. Stability of traveling waves based upon the Evans function and Legendre polynomials. Appl Sci 10;2020:846.

[42] Abdel-Gawad HI. Towards a unified method for exact Solutions of evolution Equations. An application to reaction diffusion equations with finite memory transport. J Stat Phys 2012;147:506–21.

[43] Lake BM, Yuen HC, Rungaldier H, Ferguson WE. Nonlinear deep-water waves: theory and experiment. Part 2. Evolution of a continuous wave train. J Fluid Mech 2006;83(1).

[44] El-Nabulsi RA. Nonlinear wave equation in an inhomogeneous medium from non-standard singular Lagrangians functional with two occurrences of integrals. IJNSNS 2020;21(7–8):761–6.

[45] Akhmedieva NN, Eleonskii VM, Kulagin NE. Generation of periodic trains of picoseconld pulses in an optical fiber: exact solutions. Zh Eksp Teor Fiz 89:1985; 1542-1 55 1.

[46] Carena A, Curri V, Guadino R, Poggiolini P, Benedetto S. New analytical results on fiber parametric gain and its effects on ASE noise. IEEE Photon Tech Lett 1997;9 (4):535–7.

[47] El-Nabulsi RA. The Hamilton-Jacobi analysis of powers of singular Lagrangians: A connection between the modified Schrödinger and the Navier-Stokes equations. Qual Theo Dyn Syst 2018;17:583–608.

[48] Cartaxo NN. Small-signal analysis for nonlinear and dispersive optical fibres and its application to design of dispersion supported transmission systems with optical dispersion compensation. IEE Proc – Optoelectron 1999;146(5):213–22.